JOURNAL OF MATERIALS SCIENCE 6 (1971) 118-125

The Structure of the Unidirectionally Solidified Al-AlSb Binary Eutectic

G. BEGHI, G. PIATTI, K. N. STREET*
Metallurgy and Ceramics Division CCR-Euratom, Ispra (Varese) Italy

The structures of four unidirectionally solidified A-Sb alloys of near eutectic composition were determined over a wide range of growth rates (0.6 to 49 cm/h). No cellular macrostructure was observed. At the lower solidification rates a broken lamella structure was formed; isolated grains with randomly arranged rods were also present. At higher solidification rates all grains were of the broken lamella type, more perforated and finer. With a metallographic technique it was possible to arrive at the conclusion that broken lamellae are mainly of two types: perforated lamella and branched ribbons. Crystallographic orientations were also determined; the interlamella spacing λ varied according to the relation $\lambda = AR^{-n}$, where R is the growth rate, with $n = 0.40$.

1. Introduction

It is well known that the morphology of eutectics solidified by controlled heat removal is influenced by several parameters such as rate of solidification, thermal gradient, impurities, interface energy, volume ratio of the two phases etc. The last two parameters have not been investigated to the same extent as the first three. We wish to report some observations which are primarily aimed at these two aspects.

As part of an extensive programme at CCR (Ispra) on fibre composites with an aluminium matrix the systems Al-Al_4Ca, Al-Al_4Ce, Al-Al_3Y [1] and Al-Al_2Au, Al-Al_3Pt, Al-Al_3Pd [2] have already been studied. In this paper, the results are given on the structure of several Al-Sb unidirectionally solidified alloys of near eutectic composition for a wide range of growth rates. Composition and properties of the system investigated are shown in table I.

TABLE I Characteristics of the Al-AlSb eutectic [3-5]

Solute element		Sb
Composition	wt % at. %	1.1 0.25
Phases	matrix second phase	Al AlSb
Eutectic melting point	°C	657
Second phase	melting point °C crystal structure theoretical density (g/cm^3)	~ 1065 cubic 4.34
Volume per cent eutectic %		0.84
Volume ratio of the two phases		~ 120

2. Experimental

Four alloys were prepared by resistance furnace melting under argon of the constituent elements (Al 99.99 and Sb 99.99) in Al_2O_3 crucibles. The ingots were first extruded at 500° C into the form of rods of 10 mm nominal diameter and then reduced by cold swaging to 9.5 mm final diameter. Analyses are reported in table II.

The unidirectional solidification was performed in the same equipment used for the previous studies [1, 2]. The alloy in rod form was placed in a cylindrical graphite crucible. It was then remelted and unidirectionally solidified by withdrawing the crucible from the furnace through a stationary water-spray heat sink. The solidification rate was varied between 0.6 and 49

TABLE II Analyses of the alloys

Solute element Sb (wt %)	Composition
0.6	hypoeutectic
0.9	slightly hypoeutectic
1.5	hypereutectic
5.6	hypereutectic

*Now at National Physical Laboratory, Teddington, Middx., UK

cm/h with a thermal gradient of 60 to 80° C/cm in the melt.

Metallographic examination was carried out on transverse and longitudinal sections of several specimens from each ingot. Surfaces were mechanically polished and electroetched in a solution of 6% perchloric acid in methyl alcohol. Electron microscopy by replica technique (chromium shadowed) was carried out and orientation studies were performed on several specimens by the Laue back-reflection technique.

TABLE III Al-AlSb eutectics micromorphology as function of solidification rate

Composition (Sb, wt %)	Solidification rate (R) (cm/h)	Structures
0.6 (hypoeutectic)	0.6 1.4 2.8 3.2 4.2 6.4 9.4	Coarse broken lamellae and rods Fine broken lamellae (figs. 1, 2, 3) and rods (figs. 4, 5)
	16 32	Fine broken lamellae (figs. 6, 7)
0.9 (slightly hypoeutectic)	4.2 10.5 12.3 16.5	Fine broken lamellae
1.5 (hypereutectic)	4 8	Coarse broken lamellae and irregular crystals of AlSb (fig. 8)
	17 19 22 25 30 36 42 49	Fine broken lamellae and irregular crystals of AlSb (fig. 9)
5.6 (hypereutectic)	10 14	Coarse particles of AlSb (fig. 10)

3. Results

3.1. Micromorphology

The Al-AlSb eutectic micromorphology as function of solidification rate is described in table III, from which it can be seen that:

(i) The Al-Sb eutectics are void of colonies for all the solidification rates. The lack of a cellular macrostructure over the entire range of growth rates can be attributed to the overall purity of the alloy [6, 7].

(ii) For all the considered solidification rates the hypoeutectic alloy with 0.6 wt %. Sb is characterised for the most part by a broken lamellae structure (figs. 1, 2, 4, 6, 7).

(iii) By reducing the solidification rate both the interlamellar spacing and the thickness of the broken lamellae increases. Consequently the volume of the holes, or breaks in the lamellae, is reduced, confirming previous observations [8, 9]. For this reason at low growth rates ($R \leqslant 1.4$ cm/h) the lamellae are less broken, while at higher rates ($R \geqslant 16$ cm/h) they are more perforated and finer (fig. 6).

(iv) At solidification rates between 9.4 and 0.6 cm/h randomly arranged rods were present in isolated grains (figs. 4, 5) with broken lamellae in other grains, as observed in the Pb-Ag system

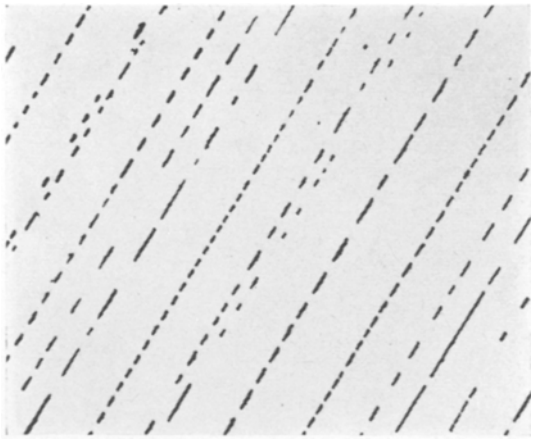

Figure 1 Al-Sb 0.6 wt% – R= 2.8 cm/h. Transverse section Broken lamellae structure (×500).

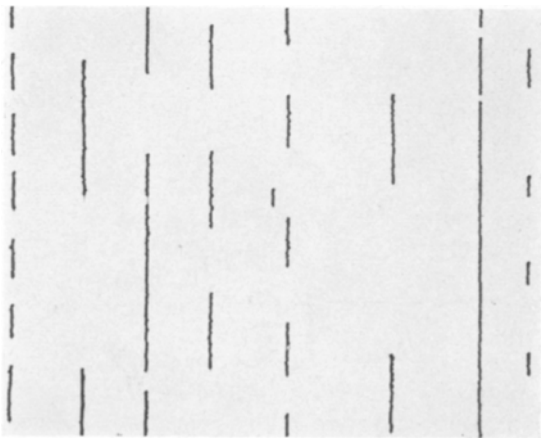

Figure 2 As in fig. 1, but longitudinal section (×500).

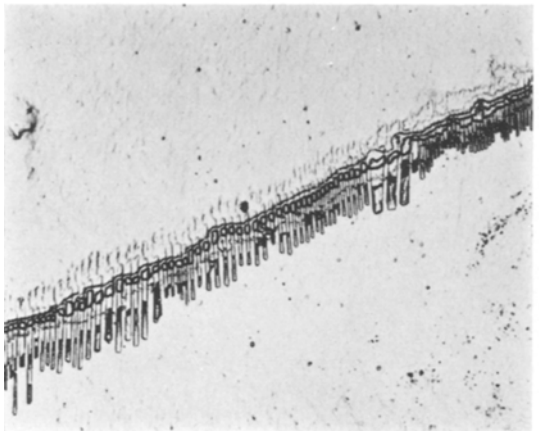

Figure 3 Al-Sb 0.6 wt % – $R = 3.2$ cm/h. Longitudinal section plane nearly parallel to broken lamella plane (×200).

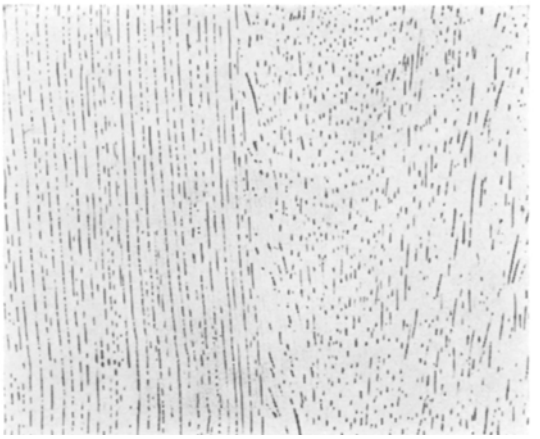

Figure 5 Al-Sb 0.6 wt % – $R = 6.4$ cm/h. Longitudinal section showing nature of slightly misaligned rods, in random rod grain (right band) (×100).

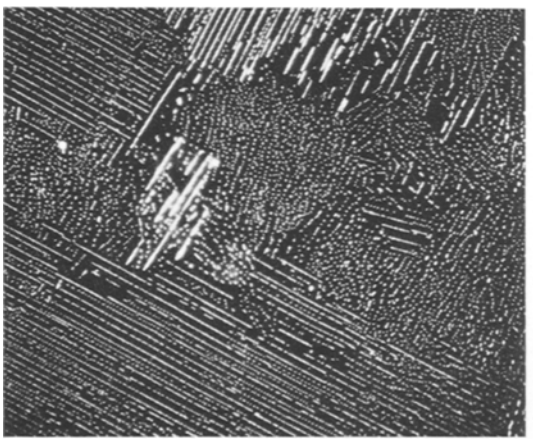

Figure 4 Al-Sb 0.6 wt % – $R = 6.4$ cm/h. Transverse section. Broken lamellae and rod like structure (dark field) (×100).

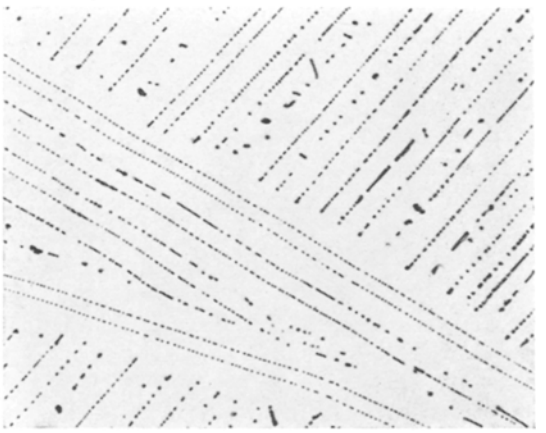

Figure 6 Al-Sb 0.6 wt % – $R = 32$ cm/h. Transverse section. Fine broken lamellae structure (×500).

[10]. At higher solidification rates ($R > 9.4$ cm/h) all grains were of the broken lamellae type.

An attempt has been made to study the morphology of a broken lamella in the eutectic using Pt wires as three-dimensional guides. The principle of the method used is shown in fig. 11. Micrographic examination of sections perpendicular to the growth axis were performed, the wires enabling one to follow a particular lamella to various depths.

Reference points consisted of two platinum wires (1 mm diameter) which had been placed parallel to the growth axis in holes drilled into the specimen, already unidirectionally solidified. From the study of micrographies of the type shown in fig. 12 it was possible to arrive at the conclusion that broken lamellae are mainly of two types: perforated lamellae and branched ribbons (fig. 13). The distinction between these categories is one of size only. Regular aligned ribbons can be ruled out. If the AlSb phase consisted of regular aligned ribbons, micrographs obtained at various depths should contain traces of constant length. This feature was not observed.

The slightly hypoeutectic 0.9 wt % Sb and the 0.6 wt % Sb alloys have a very similar structure, the only difference being that in the former the lamellae are less broken than in the latter.

A completely eutectic structure was not maintained in the hypereutectic 1.5 wt % Sb alloy. Here both fine broken lamellae and irregular

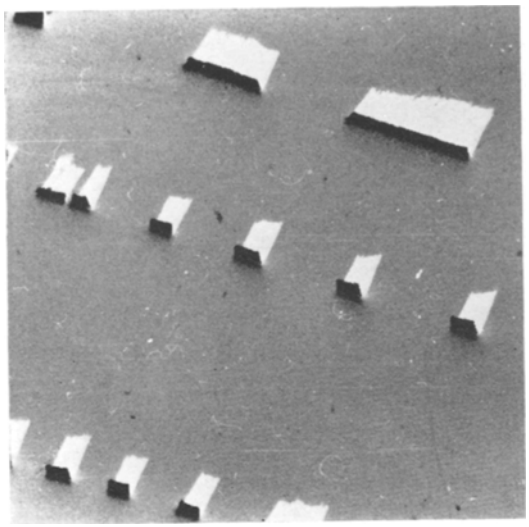

Figure 7 Al-Sb 0.6 wt % – $R = 32$ cm/h. Electron microscope replica. Broken lamellae (dark) standing proud of matrix (×4000).

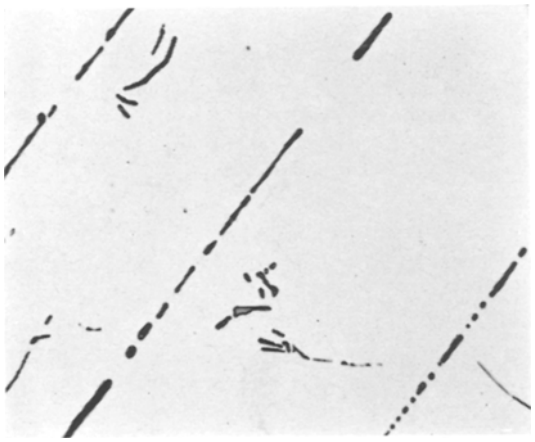

Figure 8 Al-1.5 wt % Sb – $R = 8$ cm/h. Transverse section. Coarse broken lamellae and irregular crystals of AlSb (×400).

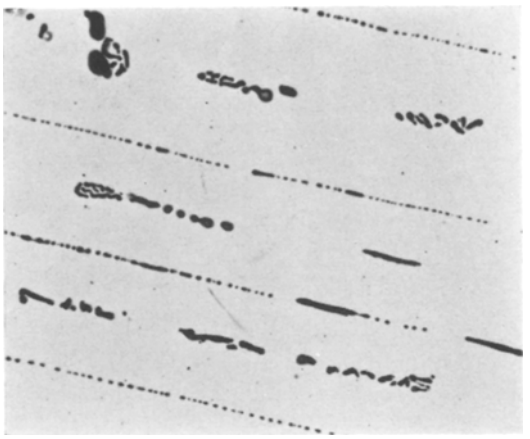

Figure 9 Al-1.5 wt % Sb – $R = 22$ cm/h. Transverse section. Fine broken lamellae and irregular crystals of AlSb (×400).

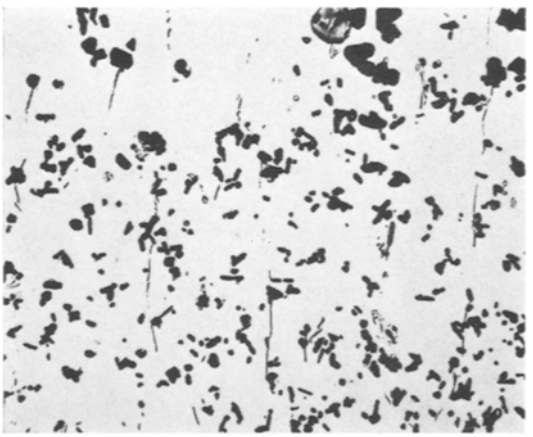

Figure 10 Al-5.6 wt % Sb – $R = 14$ cm/h. Longitudinal section. Coarse particles of AlSb (×100).

crystals within the interlamellar spacings are found (figs. 8, 9). The hypereutectic fine broken lamellae structure (thickness, interlamellar spacing, holes etc.) was found to depend on the solidification rate in the same way as the hypoeutectic alloy and hence it is not influenced at all by the AlSb primary crystals. In the 5.6 wt % Sb alloy the lamellar structure disappears altogether while large primary crystals of AlSb are found in the aluminium matrix (fig. 10).

Thus, a fully eutectic-like structure is more easily produced in hypoeutectic, rather than hypereutectic alloys, in this specific system. However, the stability range is nowhere near the wide extent observed by Mollard and Flemings for Pb-Sn [11].

The pure eutectic structure requires a stable planar solid-liquid interface and the established criterion for stability is that

$$\frac{G}{R} \geqslant -\frac{m(C_E - C_0)}{D}$$

where the symbols have the usual meaning [11]. Qualitatively the present results can be explained by the Al-Sb phase diagram [3]. The liquidus slope (m) at the eutectic composition is approxi-

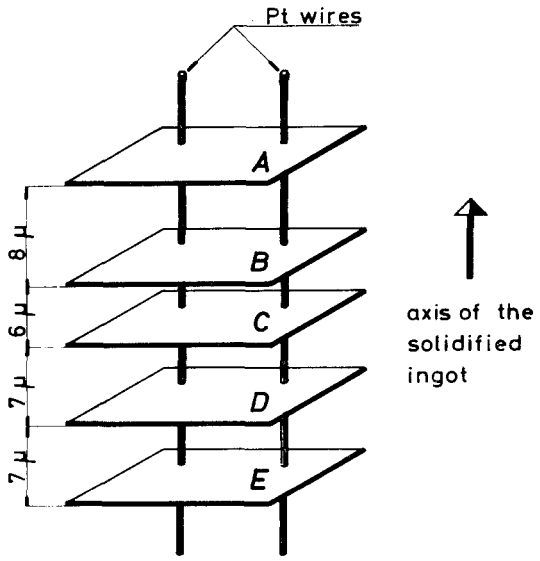

Figure 11 Schematic illustration of the Pt-wire reference point metallographic technique. A-E are the metallographic planes.

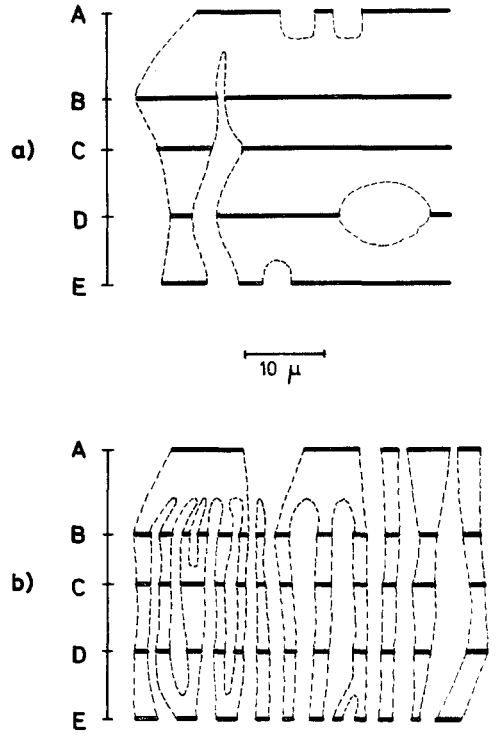

Figure 13 Examples of broken lamella morphologies derived from actual micrographs of the type shown in fig. 12. (a) Perforated lamellae. (b) Branched ribbons. A and E are the planes of sectioning.

mately seven times greater for hypereutectic alloys than for hypoeutectic alloys. Hence, a critical (G/R) value is much harder to achieve for the former. This, of course, is precisely the reason why increased volume fractions of high melting phases are extremely unlikely in eutectic alloys.

3.2. Crystallographic Orientations

Experiments were carried out to determine the orientation of the growth direction (longitudinal axis) of grains with a random structure and grains with an aligned structure using specimens of the 0.6 wt % Sb alloy. The Laue back-reflection technique was utilised. Specimens were deeply etched in aqueous HF acid and exposed to unfiltered Cu radiation. Due to the small volume percentage of the AlSb phase, only the reflections from the Al matrix were distinguished and

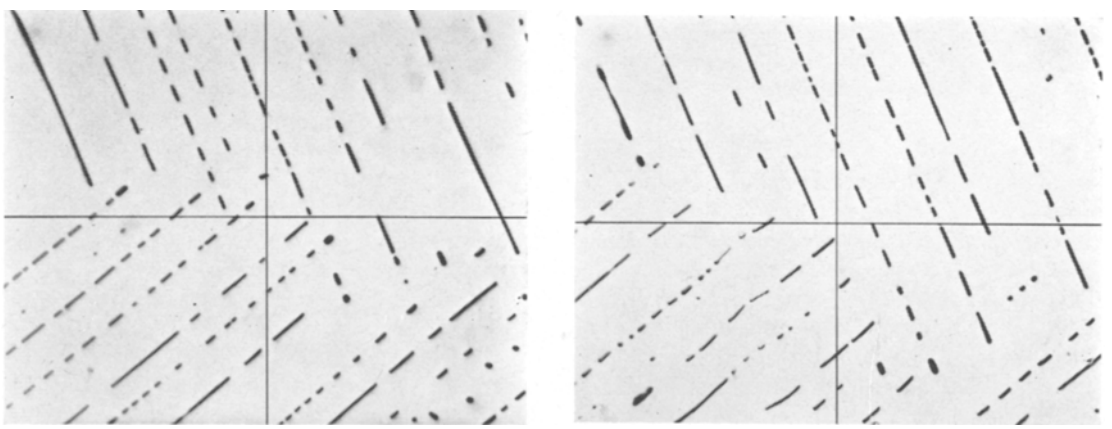

Figure 12 Examples of the micrographs executed on a specimen as indicated in fig. 11. (1) Micrograph A. (2) Micrograph E (×500).

indexed. The results are shown on a standard (001) cubic projection of Al in fig. 14. It is to be noted that the transverse sections have been taken from locations a considerable distance from the fusion line (i.e. the location in the alloy rod marking the beginning of the unidirectionally solidified structure). The aligned structure of broken lamellae or branched ribbons was formed in grains which exhibited a growth axis, close to the ⟨111⟩ direction in the Al matrix. The broken lamellae interface pole determined metallographically by the two-surface technique, coincided very closely with the ⟨111⟩ pole in the Al matrix. Kraft [10] has observed a ⟨112⟩ growth direction and {111} growth plane in the Al phase of the Al-Al_2Cu eutectic.

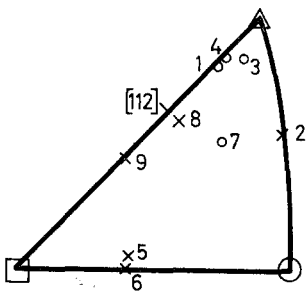

Figure 14 Orientation of growth axes of matrix grains in Al-Sb alloy (Sb 0.61 wt %).
Structure of grains:
○ broken lamellae
× random rods
Solidification rate:
R = 4 cm/h : 6 cm from fusion line: 1, 2, 3
9 cm from fusion line: 4, 5, 6
R = 9.4 cm/h : 6 cm from fusion line: 7, 8, 9
Broken lamellae interfaces parallel to (111) Al.

A verification of the tendency of the aligned structures to lie in grains where the growth axis is near ⟨111⟩ direction, is given by electron microscope observations. As shown in fig. 15, etch pits adjacent to the AlSb rods or lamellae show three-fold symmetry as expected for aluminium, in (111) planes.

Interestingly, the random rod grains exhibited more random orientations although one grain was very close to the ⟨112⟩ direction. The evidence here shows that the micromorphology of the phases in various grains is orientation dependent.

3.3. Interlamellar Spacings

Some measurements were made in order to determine whether the interphase spacing varies with the solidification rate according to the relation $\lambda = AR^{-n}$ [12, 13] where λ is the interlamellar spacing, R the solidification rate, and $n \cong 1/2$.

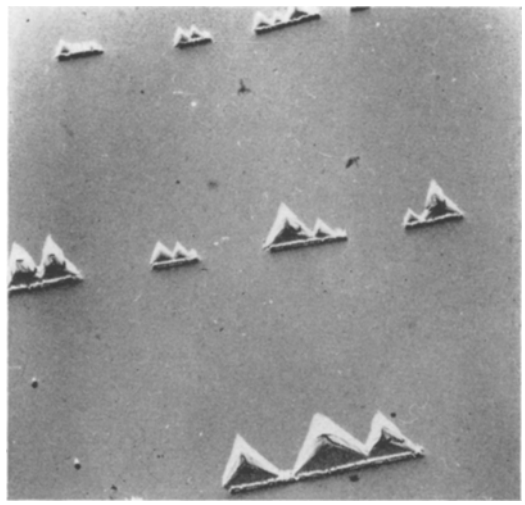

Figure 15 Electron microscope replica of broken lamellae of AlSb with adjacent triangular etch pits in Al matrix (×4100).

For the Al-0.6 wt. % Sb alloy on the basis of a logarithmic plot (fig. 16) of the average values of λ, determined by the intercept method on transversal sections, as a function of R, the value $n = 0.40$ was calculated. This lies within the range (0.30 to 0.52) as reported recently [14]. A is $2.30 \times 10^{-5}\,\mathrm{cm}^{n+1}\mathrm{h}^{-n}$.

Similar measurements were made on a limited number of specimens of Al-0.9 wt % Sb (also fig. 16). Due to the limited number of points, no line was extrapolated from these values, but we can see that they fit sufficiently well with the n value calculated for the 0.6 wt % Sb alloy. It must be noted that in the case of this alloy, λ values have large variations: sometimes λ_{max} is four or five times greater than λ_{min}. However, it appears that the average values display a linear dependence on solidification rate (log-log). λ_{min} and λ_{max} also decrease when solidification rate increases, but in more irregular fashion.

4. Discussion

The main difference between the Al-AlSb eutectic and the aluminium matrix eutectics reported earlier [1] is the smallness of the volume fraction of the intermetallic phase in the present system. We have shown that it is impossible to

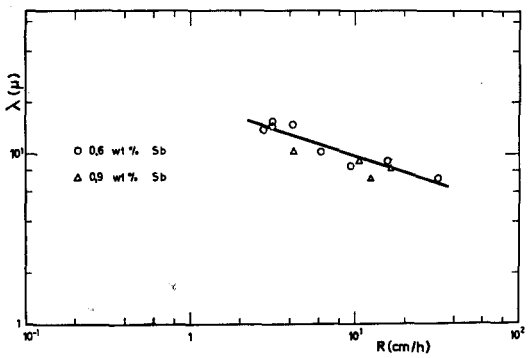

Figure 16 Logarithmic plot of the average values of interlamellar spacing (λ) as a function of solidification rate (R). $n = 0.40 - A = 2.30 \times 10^{-5}$ cm^{n+1}/h^n.

increase the AlSb content and maintain a eutectic structure by solidifying hypereutectic alloys. The thermal gradients in the melt required to maintain a eutectic structure are considered to be prohibitively high. Thus, it seems likely that composite alloys of such low volume fraction will be of interest only for their potential physical properties and not for their mechanical properties.

The focal point for discussion on broken lamellar eutectics [e.g. 15] has been the apparent lack of agreement between the predicted eutectic structures of the Jackson and Hunt theory [13] and the observed eutectic structures. Theoretical predictions are based on whether the phases grow with a faceted interface or not, but as pointed out by Chadwick [16] the propensity of a phase to form facets may depend upon whether it is in pure form (single phase material) or combined with another phase in a eutectic mixture. This dependence appears to be a very significant one. Hence, as the theoretical concepts are somewhat unclear, it seems unjustified for us to proceed along similar lines with the present alloy.

Broken lamellar eutectics contradict (on a macroscale, but not so much on a microscale) the general observation that small volume fraction systems are characterised by rod-like structures [16]. However, Jackson and Hunt [13] predict such a possibility if the surface energies are anisotropic. Our findings of the orientation dependence of the nature of Al-AlSb structures in contiguous grains (broken lamellar versus random rod) supports the existence of an anisotropic surface energy effect.

The importance of broken lamellae apparently has not been highlighted. They obviously represent a structure dictated by a long-range force favouring lamellar morphologies. However, on top of this, a short range force (instability perhaps) clearly exists which "breaks" the lamellae to the extent that they may alternatively be regarded as a rod-like structure. We shall not coin a new terminology as the eutectic literature is already fraught with an overabundance of classifications, although microstructures such as those of figs. 3, 4, and 5 might have justified a new name.

A short-range mechanism is needed to explain the breakdown of the lamellae. One possibility is that it is associated with changes in the growth direction of the eutectic as observed by Hunt and Chilton [19]. Their observations were related to macroscopic changes in direction which were found to affect the overall micromorphology of the eutectic. In the present case, this mechanism could explain the findings only if it existed at a microscopic level. It is noted that our longitudinal sections (see fig. 2) do reveal deviations in the growth direction of the AlSb phase. The source of such deviations is unknown, but it may be related to the following proposal.

The relatively large interlamellar spacings and thin lamellae found in low-volume-fraction eutectics necessitates large diffusion distances. It seems quite conceivable that thermally induced local irregularities in the solute concentration or diffusional flow in the melt could produce the irregular "breaks". Whether the significant diffusion currents are those between lamellae or along any one lamella is not obvious. The reduction in the number of breaks at low growth rates could then be due to the existence of thicker lamellae, which are less susceptible to thickness variations.

Instability has been considered from an interlamellar standpoint only [17, 18], although evidence of the type which exists in broken lamellar system (intralamellar instability) can be found in the literature, e.g. in fig. 7 of [13].

Acknowledgement

The authors are grateful to Mr E. Haine and A. Misirocchi for the experimental work.

The contribution of Mr C. F. St. John in the initial part of the work is also appreciated.

References

1. K. N. STREET, C. F. ST. JOHN, and G. PIATTI, *J. Inst. Metals* **95** (1967) 326.

2. G. BEGHI and G. PIATTI, paper presented at XIV Convegno "Associazione Italiana Metallurgia" 1970-Trieste.
3. M. HANSEN and K. ANDERKO, "Constitution of Binary Alloys" 2nd ed. (McGraw-Hill: New York, 1958).
4. W. B. PEARSON, "Lattice spacing and structures of metals and alloys" (Pergamon Press: Oxford, 1958).
5. F. A. SHUNK, "Constitution of Binary Alloys" (McGraw-Hill: New York, 1969).
6. H. W. WEART and D. J. MACK, *Trans. Met. Soc. AIME* **212** (1958) 664.
7. J. P. CHILTON and W. C. WINEGARD, *J. Inst. Metals* **89** (1960-61) 162.
8. P. J. TAYLOR, H. W. KERR, and W. C. WINEGARD, *Canad. Met. Quart.* **3** (1964) 235.
9. E. P. WHELAN and C. W. HAWORTH, *J. Austral. Inst. Met.* **12** (1967) 77.
10. E. W. KRAFT, *Trans. AIME* **224** (1962) 65.
11. F. R. MOLLARD and M. C. FLEMINGS, *ibid* **239** (1967) 1534.
12. W. A. TILLER, "Liquid Metals and Solidification" (Amer. Soc. Metals, Cleveland, Ohio, 1958).
13. K. A. JACKSON and J. D. HUNT, *Trans. AIME* **236** (1966) 1129.
14. B. L. JONES, *J. Austral. Inst. Metals* **14** (1969) 111.
15. H. W. KERR and W. C. WINEGARD, *Canad. Met. Quart.* **6** (1967) 55.
16. G. A. CHADWICK, Proc. Conf. "The solidification of Metals", Brighton, (1967) 138.
17. N. E. CLINE, *Trans. AIME* **242** (1968) 1613.
18. D. T. J. HURLE and E. JAKEMAN, Intern. Conf. on Crystal Growth, 1968.
19. J. D. HUNT and J. P. CHILTON, *J. Inst. Metals* **91** (1963) 338.

Received 18 September and accepted 17 November 1970.